Self-Assembly

DOI: 10.1002/anie.200804087

Tunable Fluorescent Dendron-Cyclodextrin Nanotubes for Hybridization with Metal Nanoparticles and Their Biosensory Function**

*Chiyoung Park, Moon Sup Im, Sanghwa Lee, Jino Lim, and Chulhee Kim**

Nanotubes are a subject of great interest because of their novel properties and potential applications in a variety of areas of nanoscience.[1,2] In particular, for organic nanotubes, the precise functionalization and interconnection of the building blocks suggested that they could exhibit not only unprecedented architectures but also valuable functions for applications such as electronics and biomedicine.[1–11]

Even though various self-assembling building blocks for nanotubes have been developed, a molecular recognition motif has not been employed for controlling the self-organization of building blocks into organic nanotubes. Recently, we have reported that cyclodextrin(CD)-covered dendron nanotubes (Den-CD-NTs) were obtained by a hierarchical self-assembly process derived from the host–guest complexation between CDs and the amide dendrons that have a focal pyrene moiety (Scheme 1).[12] Upon inclusion of the focal pyrene groups into the cavities of CDs, the smaller rim of the CD is exposed to the surface of the nanotube.

We reasoned that this type of hierarchical self-assembly approach would provide a facile methodology for the construction of diverse nanotube architectures through the host-guest interaction between the dendrons and the C6-modified CDs (Scheme 1). The tunability of the surface functionalization would enable us to construct hybrids of the nanotubes with metal nanoparticles. Furthermore, we also reasoned that the fluorescence characteristics of the nanotube in response to the change of the surface environment for the application of the nanotube could act as a biosensory vehicle.

Herein, we report a systematic approach for the construction of a series of functional nanotubes by the cooperative self-assembly of dendrons and cyclodextrins that are designed for facile control of the surface structure and specific function. Various functional groups including biological molecules such as biotin were introduced onto the tube surface by utilizing C6-modified CDs in the self-assembly process (Figure 1). In addition, nanotube–nanoparticle hybrids were constructed by using electrostatic interactions between the specific surface functionality of the tube and the precursors of metal nanoparticles. We also demonstrate a protein sensing capability of Den-CD-NTs by inducing specific binding of proteins on the tube surface. This approach shows that the Den-CD-NTs "toolkit" has a great potential for the construction of functional nanomaterials.

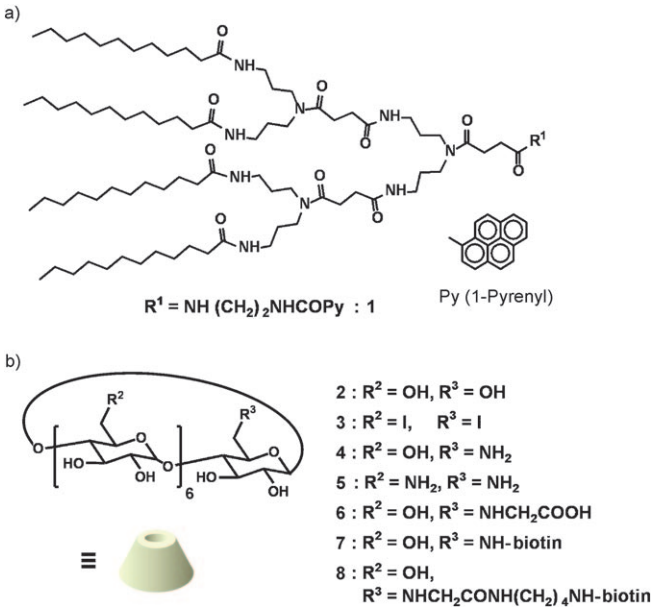

Scheme 1. Chemical structures of a) an amide dendron with a focal pyrene unit and b) functionalized cyclodextrins.

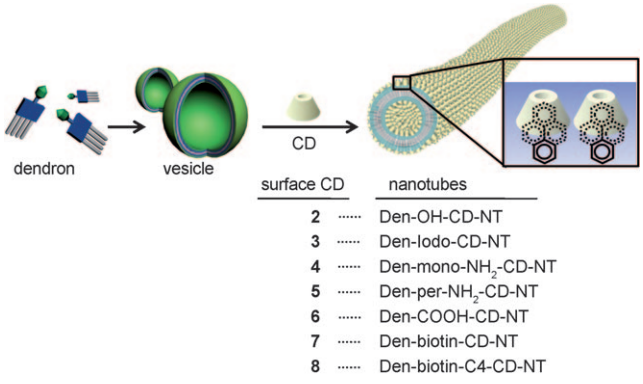

Figure 1. Nanotube "toolkit". Schematic description of the self-assembly process for the preparation of functional Den-CD-NTs.

[*] C. Park, M. S. Im, S. Lee, J. Lim, Prof. Dr. C. Kim
Department of Polymer Science and Engineering, Inha University
Incheon 402-751 (South Korea)
Fax: (+82) 32-865-5178
E-mail: chk@inha.ac.kr

[**] This work was supported by the Korea Research Foundation (2007-313-D00205), the Korea Science and Engineering Foundation grants (R01-2007-000-21031-0), and the Korea Health 21 R&D Project (A062254).

Supporting information for this article is available on the WWW under http://dx.doi.org/10.1002/anie.200804087.

The focal pyrene group was introduced into the primary building block, dendron **1**, not only as the guest moiety for the CD host but also as a fluorescent probe (Scheme 1).[12] As shown in Figure 1, dendron **1** self-organizes into vesicles in aqueous solution. Upon addition of CDs into the vesicular solution, CD–pyrene complexation occurs through the inclusion of the hydrophobic focal pyrene unit into the cavity of the CD. This supramolecular recognition transforms the self-assembled structures from the vesicle to the CD-covered nanotubes.[12] In the CD-covered nanotubes, the functional groups at the C6 position of CDs are exposed to the surface of Den-CD-NTs (Figure 1). Therefore, the utilization of C6-functionalized CDs in the self-assembly route to the nanotube is an efficient methodology for the control of the surface functionality of Den-CD-NTs. For this purpose, a functional CD library (**2**–**8**) was prepared for use as various building blocks for the supramolecular assembly (Scheme 1b; for synthetic details and characterization data, see the Supporting Information). As summarized in Figure 1, a diverse range of functional Den-CD-NTs were constructed based on the hierarchical self-assembly of dendron **1** with CDs **3**–**8** to provide iodo, amine, carboxyl, and biotin units on the surface of the tube. The functionalized nanotubes were readily constructed by addition of the modified CDs into an aqueous solution of the vesicle of dendron **1**. This solution showed a broad excimer emission of pyrene at 420–550 nm (Figure S1 in the Supporting Information). Upon addition of CDs, the excimer emission intensity of the vesicular solution of **1** was drastically reduced, and the emission of monomeric pyrene at 370–410 nm appeared because of inclusion of the pyrene moiety into the cavity of CD (Figure S1 in the Supporting Information), which induced a supramolecular transformation from the vesicles to nanotubes. The nanotubes were characterized by using transmission electron microscopy (TEM), scanning electron microscopy (SEM), and atomic force microscopy (AFM).

Figure 2 shows the representative TEM images of the nanotubes prepared from the modified CDs (Figure S2 in the Supporting Information). The diameters of the nanotubes vary from 35 to 45 nm, depending on the modified CD used for the nanotube formation. The wall thickness of the nanotubes was approximately 10.5 nm. Considering the dimension of the fully stretched structure of dendron **1** (53.5 Å), the wall thickness of the nanotube must be associated with the unilamellar bilayer of dendron **1** with the focal pyrene moiety included in the cavity of the CD. The AFM analysis also confirmed the wall thickness of the Den-CD-NTs. When a solution of Den-biotin-C4-CD-NTs was spread on a silicon wafer and dried in vacuo, AFM analysis showed that Den-biotin-C4-CD-NTs had a flattened shape (Figure 2f and Figure S2 in the Supporting Information). The height analyzed by AFM was approximately 19.7 nm, which is consistent with the double of the thickness of the bilayer of the dendron–CD complex observed in TEM experiments (Figure S2 in the Supporting Information). The bundles of the tubular structure were observed by SEM analysis (Figure S3 in the Supporting Information). The cylindrical geometry of the nanotubes in water was investigated by using dynamic light scattering (DLS). The autocorrelation functions

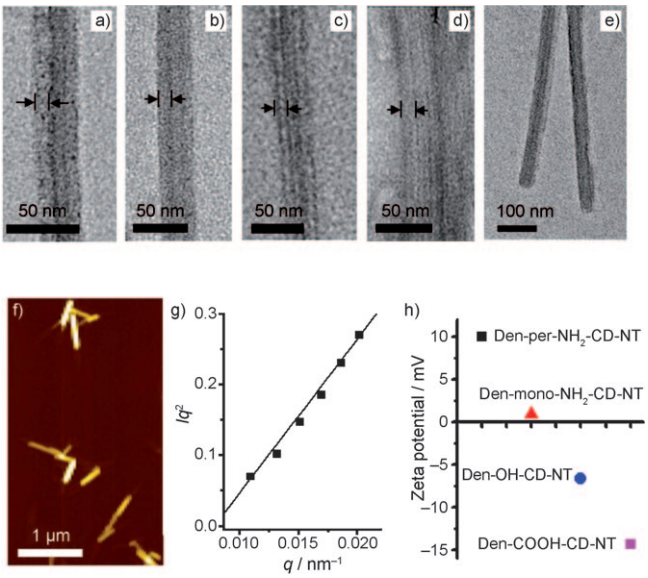

Figure 2. Functional CD-NTs. TEM images of a) Den-Iodo-CD-NTs, b) Den-per-NH_2-CD-NTs, c) Den-mono-NH_2-CD-NTs, d) Den-COOH-CD-NTs, and e) Den-biotin-C4-CD-NTs. f) AFM image of Den-biotin-C4-CD-NTs. g) Kratky plot of Den-biotin-C4-CD-NTs in aqueous solution. h) Zeta potential values of Den-CD-NTs.

acquired from the aqueous solutions of the nanotubes were analyzed by using the cumulants and CONTIN methods. The slope of the angular dependence of the apparent diffusion coefficient (D_{app}) was 0.033, which is consistent with the theoretical value predicted for cylindrical aggregates (0.03; Figure S3 in the Supporting Information).[13] Further qualitative support for the cylindrical shape was obtained from Kratky analysis of the light scattering data. The Kratky plot showed a linear angular dependence over the scattering light intensity that would be expected for cylindrical objects (Figure 2g).[13]

The C6 functionality of CDs influences the surface characteristics of Den-CD-NTs because the outer and inner surface of the nanotube is covered with CDs. We measured the zeta potentials of different nanotubes, Den-per-NH_2-CD-NTs, Den-mono-NH_2-CD-NTs, Den-COOH-CD-NTs, and β-CD-covered nanotubes (Den-OH-CD-NTs) in order to elucidate the surface charge of the nanotubes derived from modified CDs with various C6 functional groups (Figure 2h). The observed zeta potentials for Den-per-NH_2-CD-NTs (containing amino groups at all C6 positions of the CD) was 10.07 mV, while that of the Den-mono-NH_2-CD-NTs (with only one amino group on the CD) was 0.96 mV. Den-COOH-CD-NTs (covered with carboxylic acids) showed a potential of −14.36 mV, and the surface of Den-OH-CD-NTs gave a zeta potential of −6.67 mV. These results clearly demonstrate that our hierarchical self-assembly approach provides a facile route to the functional nanotubes derived from dendrons and the C6-modified CDs.

The tunability of the nanotube surface functional groups should lead to an opportunity for the construction of nanostructures for further applications.[1,5,14–17] We designed a hybrid assembly of nanoparticles with the nanotube templates that have the surface functional groups to accommodate

metal nanoparticles. Two different design approaches were employed. The first approach was the assembly of gold nanoparticles (AuNPs) onto the surface of the Den-CD-NTs template. This was achieved by the electrostatic interaction between anionic AuNPs and Den-mono-NH_2-CD-NTs which has a cationic surface (Figure 3a). Den-mono-NH_2-CD-NTs was incubated with AuNPs that were passivated with 3-mercaptoacetic acid (AuNP-COOH, average diameter: (1.7 ± 0.3) nm; Figure S4 in the Supporting Information). The binding of AuNP-COOH onto the surface of Den-mono-NH_2-CD-NTs led to a drastic quenching of the pyrene emission (ca. 85% fluorescence quenching efficiency) because of photoinduced electron transfer from the pyrene units to proximate AuNPs (Figure 3b).[18] The TEM image in Figure 3c shows that the surface of Den-mono-NH_2-CD-NTs is well-covered with AuNP-COOH. In case of Den-per-NH_2-CD-NTs, derived from the self-assembly of CD **5** and dendron **1**, the amino groups on the surface facilitated the binding of AuNP-COOH on Den-per-NH_2-CD-NTs. As expected, the TEM image of the Au/Den-per-NH_2-CD-NTs hybrid showed that AuNP-COOH was densely coated on the tube surface, and then the degree of the fluorescence quenching efficiency of pyrene emission was approximately 94% (Figure S4 in the Supporting Information). In contrast, as a negative control, TEM analysis showed that addition of AuNP-COOH into a solution of Den-OH-CD-NTs did not result in the assembly of AuNP-COOH on the surface of the Den-OH-CD-NTs, which indicates that AuNP-COOH and Den-OH-CD-NTs do not interact strongly. Consequently, no significant fluorescence quenching was observed.

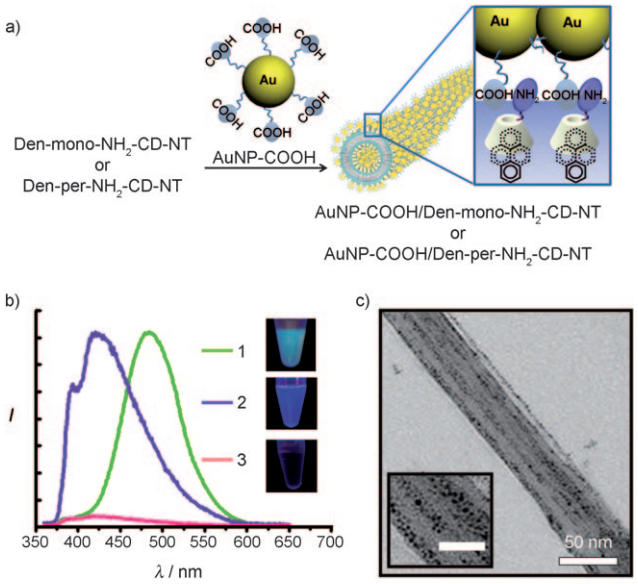

Figure 3. a) Orientation of metal nanoparticles on the surface of fluorescent Den-CD-NTs. b) Fluorescence spectra of 1) vesicle of dendron **1**, 2) Den-mono-NH_2-CD-NTs, and 3) AuNP-COOH/Den-mono-NH_2-CD-NTs. c) TEM image and enlarged TEM image (scale bar of inset: 20 nm) of AuNP-COOH/Den-mono-NH_2-CD-NTs.

As a second approach to generate the hybrid of Den-CD-NTs and metal nanoparticles, we attempted a direct growth of metal nanoparticles on the surface of Den-CD-NTs (Figure 4a). The precursor of metal nanoparticles can be adsorbed on the surface of the Den-mono-NH_2-CD-NTs template by electrostatic interactions under appropriate conditions.

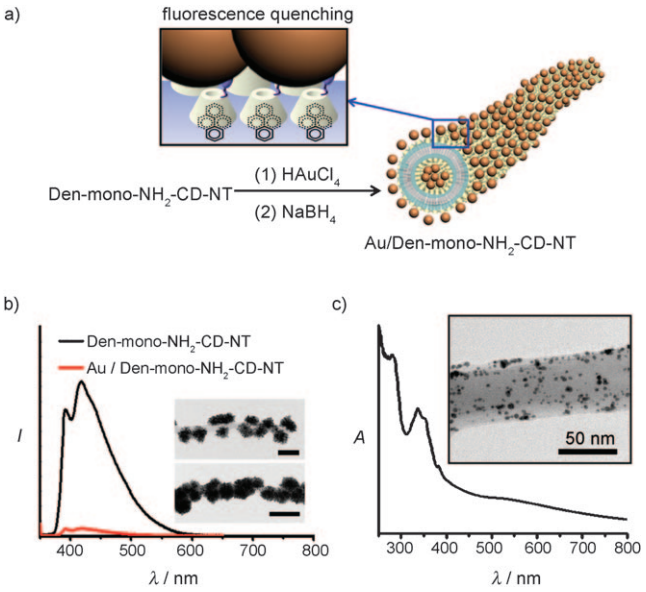

Figure 4. a) Schematic description showing the preparation of nanotube–nanoparticle hybrids. b) Fluorescence spectra of Den-mono-NH_2-CD-NTs and Au/Den-mono-NH_2-CD-NTs ([Den-mono-NH_2-CD-NT] = 5.6 μg mL^{-1}). The inset shows TEM images of Au/Den-mono-NH_2-CD-NTs ([Den-mono-NH_2-CD-NTs] = 5.6 μg mL^{-1}, scale bars: 50 nm and 100 nm, respectively). c) Absorption spectra of Au/Den-mono-NH_2-CD-NTs ([Den-mono-NH_2-CD-NTs] = 0.4 mg mL^{-1}) in the aqueous phase. The inset shows TEM images of Au/Den-mono-NH_2-CD-NTs ([Den-mono-NH_2-CD-NTs] = 0.4 mg mL^{-1}).

Subsequent reduction would result in formation of the nanoparticles on the surface of Den-mono-NH_2-CD-NTs. The tubes with different surface functional groups exhibited selective adsorption behavior towards metal nanoparticle precursors, as described here for Au nanoparticles. The tubes with a cationic surface, Den-mono-NH_2-CD-NTs, can accommodate anionic metal precursors. For example, incubation of Den-mono-NH_2-CD-NTs (5.6 μg mL^{-1}) in water with the anionic $[AuCl_4]^-$ precursor ($HAuCl_4$, 0.4 mM, 20 μL) followed by gradual reduction ($NaBH_4$, 0.6 mM, 20 μL) resulted in the formation of Au nanoparticles on Den-mono-NH_2-CD-NTs (Au/Den-mono-NH_2-CD-NTs). After reduction, the Au/Den-mono-NH_2-CD-NTs solution exhibited pale pink-red color. The TEM images in Figure 4b show that Au/Den-mono-NH_2-CD-NTs are densely covered with Au particles, which was further confirmed by energy-dispersive X-ray (EDX) analysis, which indicated the presence of Au, C, N, and O in Au/Den-mono-NH_2-CD-NTs (Figure S5 in the Supporting Information). The UV/Vis spectrum of a solution of Au/Den-mono-NH_2-CD-NTs shows a weak surface plasmonic band around 580 nm derived from the Au nanoparticle (Figure S5 in the Supporting Information). However, no absorption was observed around 580 nm from a solution of Den-mono-NH_2-CD-NTs, which does not contain Au particles. The dense

coverage and aggregation of Au nanoparticles on the Den-mono-NH_2-CD-NTs surface result in a red shift and broadening of the plasmon band associated with the Au nanoparticles.[19] The fluorescence spectra in Figure 4b show that the pyrene emission from Den-mono-NH_2-CD-NTs appeared between 370–600 nm, which was quenched in Au/Den-mono-NH_2-CD-NTs with an efficiency of approximately 95% because of the proximity of the pyrene units and the Au nanoparticles (Figure 4a).[18,20] We found that the size of the nanoparticles on the Den-mono-NH_2-CD-NTs could be controlled depending on the amount of the Au salt used in the reaction. The TEM image in Figure 4c shows that Au/Den-mono-NH_2-CD-NTs ([Den-mono-NH_2-CD-NT] = 0.4 mg mL^{-1}) are covered with Au particles with an average diameter of about 4 nm; the weak absorption band around 520 nm of Au/Den-mono-NH_2-CD-NTs in Figure 4c arises from the surface plasmon absorption of the Au nanoparticles. These results confirm the binding of Au nanoparticles on the surface of Den-mono-NH_2-CD-NTs. A control experiment using Den-COOH-CD-NTs with $HAuCl_4$ revealed that Au nanoparticles were poorly adsorbed onto the nanotube that does not have a cationic surface for anchoring the anionic precursor (Figure S6 in the Supporting Information). This result indicates that the nature of the surface functional group is critical for the formation of specific metal nanoparticles on Den-CD-NTs. In the case of the reduced solution of CD **4** and $HAuCl_4$, we observed extensive aggregation among Au nanoparticles (Figure S6 in the Supporting Information).

The fluorescent nature of Den-CD-NTs with a tunable surface functionality provides an opportunity for utilizing the nanotubes as a biosensing platform when the surface functional groups of the nanotubes are designed to interact specifically with the analytes. The sensitive emission of the pyrene units in the cavity of the CDs towards the change in local environment would allow binding of the biomolecules on the nanotubes to trigger a change in their fluorescence emission. We prepared biotin-covered nanotubes (Den-biotin-CD-NTs and Den-biotin-C4-CD-NTs) as biosensing platforms for utilizing the specific binding of biotin with receptor proteins such as streptavidin and avidin. The binding of fluorescein-labeled streptavidin (SA-FITC) on the surface of Den-biotin-CD-NTs and Den-biotin-C4-CD-NTs was visualized by confocal laser scanning microscopy (CLSM) after addition of SA-FITC into the solutions of Den-biotin-CD-NTs or Den-biotin-C4-CD-NTs (Figure 5a and b). Networks of the fibrous structures, that is, bundles of the SA-FITC bound nanotubes, were observed by CLSM. However, no noticeable fibrous images were observed from the mixture of SA-FITC with the OH-covered nanotube, Den-OH-CD-NTs, by CLSM. Similarly, when the biotin binding sites of SA-FITC were presaturated with biotin prior to mixing with Den-biotin-CD-NTs, no fibrous structures were observed by CLSM. These results indicate that the fibrous image of Den-biotin-CD-NTs/SA-FITC and Den-biotin-C4-CD-NTs/SA-FITC shown in Figure 5a,b was obtained as a result of specific binding of SA-FITC to the biotin moiety on the surface of Den-biotin-CD-NTs and Den-biotin-C4-CD-NTs. In addition, when the streptavidin–AuNP conjugate (SA–AuNP) was added to the Den-biotin-C4-CD-NTs solution,

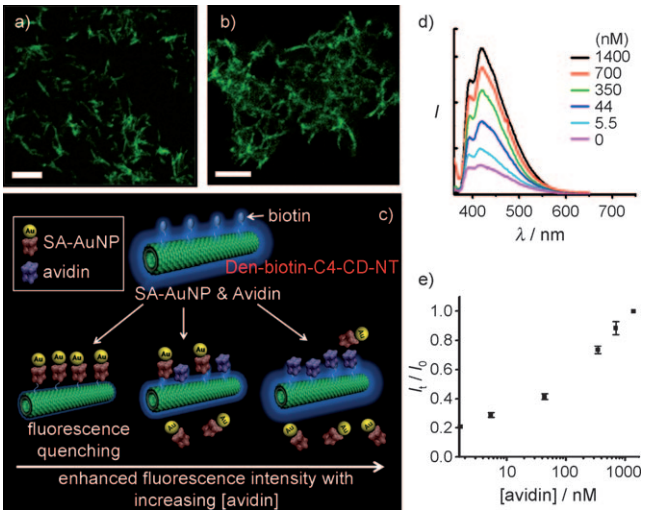

Figure 5. Detection of proteins using fluorescent Den-CD-NT templates. a) SA-FITC/Den-biotin-CD-NTs and b) SA-FITC/Den-biotin-C4-CD-NTs (scale bar: 5 μm). c) Schematic representation of the inhibition assay on Den-biotin-C4-CD-NTs. d) Fluorescence spectra of Den-biotin-C4-CD-NTs and SA-Au NP/Den-biotin-C4-CD-NTs. e) I_t/I_0 ratio of SA-AuNP/Den-biotin-C4-CD-NTs as a function of avidin concentration.

the fluorescence was quenched because of the proximity of the pyrene moieties to the AuNPs of SA-AuNP, which bind to the biotin unit on the tube surface. These fluorescence characteristics of the Den-CD-NTs together with well-defined surface architecture suggest that Den-CD-NTs can be utilized as a biosensor. To demonstrate the possibility of Den-CD-NTs as a biosensory vehicle, an inhibition assay was carried out between streptavidin, avidin, and biotin as a proof-of-concept experiment.[21] The sensing system consists of three components: 1) Den-CD-NTs as a sensory machine with fluorescence probes and biotin ligands for sensing proteins, 2) SA-AuNPs as a fluorescence quencher, and 3) avidin as a target protein (Figure 5c). As shown in Figure 5d, upon addition of SA-AuNP into the Den-biotin-C4-CD-NTs solution, the fluorescence of Den-biotin-C4-CD-NTs was quenched because the SA-AuNPs became bound to the biotin moiety on the surface of Den-biotin-C4-CD-NTs to form the hybrid (SA-AuNPs/Den-biotin-C4-CD-NTs). The fluorescence intensity of Den-biotin-C4-CD-NTs was reduced by increasing the amount of SA-AuNP added to the solution. A negative control experiment was carried out to rule out the possibility of fluorescence quenching by nonspecific binding of SA-AuNPs on the nanotube or by unbound SA-AuNP. The addition of SA-AuNPs, the binding sites of which were presaturated with biotin, did not result in fluorescence quenching. In addition, when avidin-saturated Den-biotin-C4-CD-NTs was incubated with SA-AuNP, the fluorescence of avidin-saturated Den-biotin-C4-CD-NTs was not changed (Figure S7 in the Supporting Information). These results indicate that the fluorescence behavior of Den-biotin-C4-CD-NTs is due to the specific binding of SA-AuNP to the biotin on the surface of Den-biotin-C4-CD-NTs rather than nonspecific binding between the protein and the nanotube.

In the inhibition assay with Den-biotin-C4-CD-NTs, SA-AuNP, and avidin, the fluorescence intensity of pyrene in

Den-biotin-C4-CD-NTs increased with increasing concentration of avidin, because SA-AuNP binds less strongly to biotin than avidin; thus the concentration of SA-AuNPs bound on Den-biotin-C4-CD-NTs decreases with increasing avidin concentration. As shown in Figure 5e, the I_t/I_0 ratio increased with increasing avidin concentration (I_0 denotes the fluorescence intensity of Den-biotin-C4-CD-NTs, and I_t is the fluorescence intensity of SA-AuNP/Den-biotin-C4-CD-NTs depending on the avidin concentration). The detection limit for avidin was in the range of approximately 1 nM.

In summary, we have prepared a series of functional Den-CD-NTs derived from self-assembly of dendritic building blocks. The structure of Den-CD-NTs can be controlled in a facile way by using the modified CDs in the supramolecular transformation process from vesicle to nanotube. The surface structure of Den-CD-NTs is tunable through the use of C6-modified CDs because the tube surface is covered with CDs. Furthermore, the Den-CD-NTs with functionally controllable surfaces can be utilized as useful tools for the construction of nanotube–nanoparticle hybrid assemblies, supramolecular biological assemblies, and biomolecular sensors. The substantial advantage of our supramolecular approach to functional nanomaterials has been demonstrated by tunability of the structure and function of Den-CD-NTs, which can thus provide new insights in nanotechnology and supramolecular chemistry.

Received: August 19, 2008
Published online: November 10, 2008

Keywords: biosensors · cyclodextrins · dendrons · nanotubes · self-assembly

[1] T. Shimizu, M. Masuda, H. Minamikawa, *Chem. Rev.* **2005**, *105*, 1401 – 1444.
[2] X. Gao, H. Matsui, *Adv. Mater.* **2005**, *17*, 2037 – 2050.
[3] J. L. Mynar, T. Yamamoto, A. Kosaka, T. Fukushima, N. Ishii, T. Aida, *J. Am. Chem. Soc.* **2008**, *130*, 1530 – 1531.
[4] N. Kameta, M. Masuda, H. Minamikawa, Y. Mishima, I. Yamashita, T. Shimizu, *Chem. Mater.* **2007**, *19*, 3553 – 3560.
[5] Y. Zhou, T. Shimizu, *Chem. Mater.* **2008**, *20*, 625 – 633.
[6] J. P. Hill, W. Jin, A. Kosaka, T. Fukushima, H. Ichihara, T. Shimomura, K. Ito, T. Hashizume, N. Ishii, T. Aida, *Science* **2004**, *304*, 1481 – 1483.
[7] Y. Yamamoto, T. Fukushima, Y. Suna, N. Ishii, A. Saeki, S. Seki, S. Tagawa, M. Taniguchi, T. Kawai, T. Aida, *Science* **2006**, *314*, 1761 – 1764.
[8] J. M. Schnur, *Science* **1993**, *262*, 1669 – 1676.
[9] G. C. L. Wong, J. X. Tang, A. Lin, Y. Li, P. A. Janmey, C. R. Safinya, *Science* **2000**, *288*, 2035 – 2039.
[10] S. Fernandez-Lopez, H.-S. Kim, E. C. Choi, M. Delgado, J. R. Granja, A. Khasanov, K. Kraehenbuehl, G. Long, D. A. Weinberger, K. M. Wilcoxen, M. R. Ghadiri, *Nature* **2001**, *412*, 452 – 455.
[11] D. T. Bong, T. D. Clark, J. R. Granja, M. R. Ghadiri, *Angew. Chem.* **2001**, *113*, 1016 – 1041; *Angew. Chem. Int. Ed.* **2001**, *40*, 988 – 1011.
[12] C. Park, I. H. Lee, S. Lee, Y. Song, M. Rhue, C. Kim, *Proc. Natl. Acad. Sci. USA* **2006**, *103*, 1199 – 1203.
[13] M. Schmidt, W. H. Stockmayer, *Macromolecules* **1984**, *17*, 509 – 514.
[14] M. Reches, E. Gazit, *Science* **2003**, *300*, 625 – 627.
[15] E. D. Sone, E. R. Zubarev, S. I. Stupp, *Angew. Chem.* **2002**, *114*, 1781 – 1785; *Angew. Chem. Int. Ed.* **2002**, *41*, 1705 – 1709.
[16] L. M. Li, E. Beniahs, E. R. Zubarev, W. H. Xiang, B. M. Rabatic, G. Z. Zhang, S. I. Stupp, *Nat. Mater.* **2003**, *2*, 689 – 694.
[17] I. A. Banerjee, L. Yu, H. Matsui, *Proc. Natl. Acad. Sci. USA* **2003**, *100*, 14678 – 14682.
[18] B. I. Ipe, K. G. Thomas, S. Barazzouk, S. Hotchandani, P. V. Kamat, *J. Phys. Chem. B* **2002**, *106*, 18 – 21.
[19] Z. Li, S. W. Chung, J. M. Nam, D. S. Ginger, C. A. Mirkin, *Angew. Chem.* **2003**, *115*, 2408; *Angew. Chem. Int. Ed.* **2003**, *42*, 2306.
[20] C. Fan, S. Wang, J. W. Hong, G. C. Bazan, K. W. Plaxco, A. J. Heeger, *Proc. Natl. Acad. Sci. USA* **2003**, *100*, 6297.
[21] E. Oh, M.-Y. Hong, D. Lee, S.-H. Nam, H. C. Yoon, H.-S. Kim, *J. Am. Chem. Soc.* **2005**, *127*, 3270 – 3271.

